

This is the accepted manuscript made available via CHORUS. The article has been published as:

Single-atom gating and magnetic interactions in quantum corrals

Anh T. Ngo, Eugene H. Kim, and Sergio E. Ulloa

Phys. Rev. B **95**, 161407 — Published 19 April 2017

DOI: [10.1103/PhysRevB.95.161407](https://doi.org/10.1103/PhysRevB.95.161407)

Single-atom gating and magnetic interactions in quantum corrals

Anh T. Ngo,^{1,2} Eugene H. Kim,³ and Sergio E. Ulloa²

¹*Materials Science Division, Argonne National Laboratory, 9700 S. Cass Ave., Argonne, IL 60439, USA.*

²*Department of Physics and Astronomy, and Nanoscale and Quantum Phenomena Institute, Ohio University, Athens, OH 45701*

³*Department of Physics, University of Windsor, Windsor, ON, Canada N9B 3P4*

Single-atom gating, achieved by manipulation of adatoms on a surface, has been shown in experiments to allow precise control over superposition of electronic states in quantum corrals. Using a Green's function approach, we demonstrate theoretically that such atom gating can also be used to control the coupling between magnetic degrees of freedom in these systems. Atomic gating enables control not only on the direct interaction between magnetic adatoms, but also over superpositions of many-body states which can then control long distance interactions. We illustrate this effect by considering the competition between direct exchange between magnetic impurities and the Kondo screening mediated by the host electrons, and how this is affected by gating. These results suggest that both magnetic and nonmagnetic single-atom gating may be used to investigate magnetic impurity systems with tailored interactions, and may allow the control of entanglement of different spin states.

There is considerable interest in readily controlling the spin degree of freedom of atoms and electrons in order to explore their dynamical behavior under different situations. It has also been suggested that one could use the spin in electronic and information devices,^{1,2} as this creates possibilities for new technologies. The continuing drive to miniaturize devices,³ further introduces interesting quantum effects at the reduced length scales. In particular, the availability and delicate control of scanning probes at the nanometer scale has opened new areas of inquiry where magnetic moments and quantum effects may play important roles.⁴

Atomic manipulation with scanning tunneling microscopes (STM) has indeed allowed the design and probing of nanometer scale systems to explore their quantum behavior. Prominent among these are quantum corrals defined by arrangements of atoms on metallic surfaces in different geometries.⁵ Such structures have been used to explore interesting concepts and phenomena, including propagation of information,⁶ Kondo “mirages” in elliptical corrals,^{7–9} and quantum manipulation using spin-orbit coupling effects.^{10,11} Work in related structures has also demonstrated the ability to create quantum superposition of states using single atoms as “movable gates” in a structure, as controlling the location of atoms allows for mixing of degenerate states.¹² Changing the location of single styrene-based molecules with respect to charged dangling bonds on a surface has allowed control of the conductance through the molecule, showing that the electrostatic environment can be used to regulate the conductivity of an active species.¹³ Recent work with phthalocyanine molecules has clearly demonstrated the gating of single-molecule “transistors” by manipulating the location of charged ions in the proximity of the molecule, all with nanometer precision.¹⁴

Motivated by this work, we present here our theoretical studies on the control of the interaction between magnetic impurities in an elliptical quantum corral. We demonstrate that by choosing the location and charac-

teristics of a gating single atom, it is possible to dramatically modify the effective exchange interaction between magnetic adatoms in such system. We also explore and demonstrate how the resulting configuration (such as the strength and features of a Kondo mirage) can be modified by introduction of single-atom gates. We show that suitable placement of the gating atom can directly affect the competition for the ground state configuration of multiple magnetic adatoms. In particular, we analyze how the Kondo screening of single impurities in the quantum corral is dominated by the indirect exchange of nearby impurities. These results demonstrate that one could indeed implement rather exquisite control over the coupling between magnetic degrees of freedom and superposition of many-body states over distances of tens of nanometers. These attractive and tantalizing results may be applicable in different quantum structure systems.¹⁵

Our system includes a quantum corral (QC) built on the two-dimensional electron gas (2DEG) of a metallic surface by adatoms located along an elliptical shape that defines it. To describe the QC, we consider the Hamiltonian

$$H_{QC} = \int d\mathbf{r} \, \psi_s^\dagger(\mathbf{r}) \left[\frac{1}{2m^*} \mathbf{p}^2 + V(\mathbf{r}) \right] \psi_s(\mathbf{r}) , \quad (1)$$

where $\psi_s(\mathbf{r})$ is the 2D electron field operator for spin- s —we implicitly sum over spin indices—and \mathbf{r} and \mathbf{p} are the electron's position and momentum operators, with effective mass m^* . $V(\mathbf{r})$ is the potential describing the QC's elliptical wall. We are interested in the system's low-energy properties, and treat the atoms making up the QC's wall as a collection of s -wave scatterers^{16,17}

$$V(\mathbf{r}) = V_0 \sum_i \delta(\mathbf{r} - \mathbf{r}_i) , \quad (2)$$

where V_0 parameterizes the s -wave scattering phase shift, and the atoms defining the ellipse are located at positions $\{\mathbf{r}_i\}$. For simplicity, we take the s phase shift to be

purely imaginary, as the results we report are found to be robust to changes in the phase shift, having only quantitative effects, leaving the overall physical discussion and conclusions unaffected.¹⁷ As we will describe below, we use a Green's function formalism to extract information on the system.

We will focus results on an elliptical QC defined by 40 atoms regularly spaced along the ellipse, similar to what has been realized experimentally,^{7,12} and described by $(x/a)^2 + (y/b)^2 = 1$ with $b=57.2\text{\AA}$, $a/b=1.5$, and $(\pm c, 0)$ being the ellipse's foci, $c = \sqrt{a^2 - b^2} = 63.9\text{\AA}$. We further consider physical values of the parameters of the 2DEG relevant to the surface of Cu(111), with 2D Fermi energy $E_F=0.45\text{eV}$ and $m^*=0.38m_e$ (m_e is the bare electron mass).¹¹

As noted above, we are interested in using magnetic atoms to explore their interaction inside the QC, and how this is affected by single-atom gating. To describe the coupling of magnetic adatoms to the surface 2DEG, we consider a local exchange Hamiltonian,¹⁸ where each of two magnetic impurities interacts with the electrons in the host via

$$H_{\text{sd}} = J \vec{\tau}_1 \cdot \mathbf{S}(\mathbf{R}_1) + J \vec{\tau}_2 \cdot \mathbf{S}(\mathbf{R}_2), \quad (3)$$

where $\vec{\tau}_i$ is the spin-operator for impurity- i , and $\mathbf{S}(\mathbf{R})$ is the 2DEG's spin density operator at \mathbf{R} , $\mathbf{S}(\mathbf{R})=(1/2)\psi_s^\dagger(\mathbf{R})\vec{\sigma}_{s,s'}\psi_{s'}(\mathbf{R})$ with $\{\sigma^\mu\}$ being the Pauli matrices. We take $J > 0$, as expected for the antiferromagnetic coupling between a magnetic adatom and the metallic host,¹⁸ and for simplicity assume the magnetic adatoms to have spin-1/2 moment.³³

When placed in a metallic host, a magnetic atom experiences screening of its magnetic moment by the host electrons. This many-body effective antiferromagnetic correlation between the magnetic atom and the surrounding electrons is characterized by an energy scale, the Kondo temperature T_K , such that many properties of the system are drastically affected for temperatures below T_K .¹⁸ In particular, the Kondo effect gives rise to a resonance in the spectral function (electronic density of states) at or near the Fermi energy, (the Kondo or Abrikosov-Suhl-Nagaoka resonance), which has been detected in a variety of systems by differential conductance studies in STM experiments.^{19,20} Interestingly, the Kondo resonance has been used as a 'signal source' or electronic beacon which can be projected across the system. This concept was demonstrated in beautiful experiments that showed that the Kondo resonance of a magnetic adatom at one of the foci in a QC could indeed be projected across to the other (empty) focus, and give rise to a non-zero differential conductance signal there.⁷ We explore below how a second atom in the system (magnetic or not) can provide further control of such signal.

It is also important to consider that whenever two magnetic adatoms are placed in the metallic host, as would be the case in Eq. (3), the electrons may also mediate an effective exchange interaction between impurities. This Ruderman-Kittel-Kasuya-Yosida (RKKY) interaction is

long-ranged (as it decays as the square of the impurity separation for this 2D system), and changes sign (oscillates between anti- and ferromagnetic character)) with a wavelength of half the Fermi wavelength in the host.²¹ This interaction has been explored at the atomic level in different STM experiments, including engineered atomic structures.²²⁻²⁴ Most interestingly, there is a clear competition between the RKKY and Kondo interactions, which depends critically on the relative impurity separation and strength of different couplings. This competition has been studied in detail in different systems, both theoretically and experimentally.²⁵⁻²⁷ As we will demonstrate below, single-atom gating may also strongly affect this competition, and as such, provide a unique tool to control the relative effect of many-body screening effects.

The RKKY interaction can be obtained after integrating out the 2DEG's degrees of freedom.²⁸ Upon doing this, the effective interaction between impurities is written as

$$H_{\text{RKKY}} = K \vec{\tau}_1 \cdot \vec{\tau}_2, \quad (4)$$

with

$$K = -\frac{J^2}{\pi} \int_0^{E_F} d\omega \text{Im} [G_0(\mathbf{R}_1, \mathbf{R}_2; \omega) G_0(\mathbf{R}_2, \mathbf{R}_1; \omega)] , \quad (5)$$

where E_F is the Fermi energy of the 2DEG. Here, $G_0(\mathbf{r}, \mathbf{r}'; \omega)$ is the retarded Green's function (GF) of the QC in the absence of the magnetic impurities (i.e. with $J=0$). It is determined by the Dyson equation

$$G_0(\mathbf{r}, \mathbf{r}'; \omega) = G_{00}(\mathbf{r}, \mathbf{r}'; \omega) + \sum_i G_{00}(\mathbf{r}, \mathbf{r}_i; \omega) V_0 G_0(\mathbf{r}_i, \mathbf{r}'; \omega), \quad (6)$$

with $G_{00}(\mathbf{r}, \mathbf{r}'; \omega)$ denoting the free-particle GF, i.e. the GF in the absence of the QC's wall and impurities [$G_{00}(\mathbf{r}, \mathbf{r}'; \omega) \propto H_0(|\mathbf{r} - \mathbf{r}'| \sqrt{2m^*\omega})$, where $H_0(z)$ is a Hankel function.²⁹] Previous work has discussed control of the RKKY interaction in different shape QCs and the consequent spin correlations.³⁰

Let us first explore the role of the QC on the RKKY between impurities. Figure 1a shows the interaction between two magnetic impurities, where one atom is fixed at the focus $(-c, 0)$ while the other is moved away along the long axis of the ellipse (the x -direction). As mentioned, this interaction arises from the spin polarization induced in the 2DEG by one of the adatoms and communicated to the other by the host electrons, inducing an effective long-range interaction between the adatoms.²⁸ It is clear that the QC reduces the amplitude of the interaction (see red curve), and shifts the phase of the oscillations by $\approx \pi/2$.

Figure 1b shows the effect of a single *nonmagnetic* atom introduced as gate, which modifies the effective spin interaction by disturbing the charge density inside the QC. The curve shows the resulting RKKY interaction when the two magnetic impurities are fixed at 1 nm from

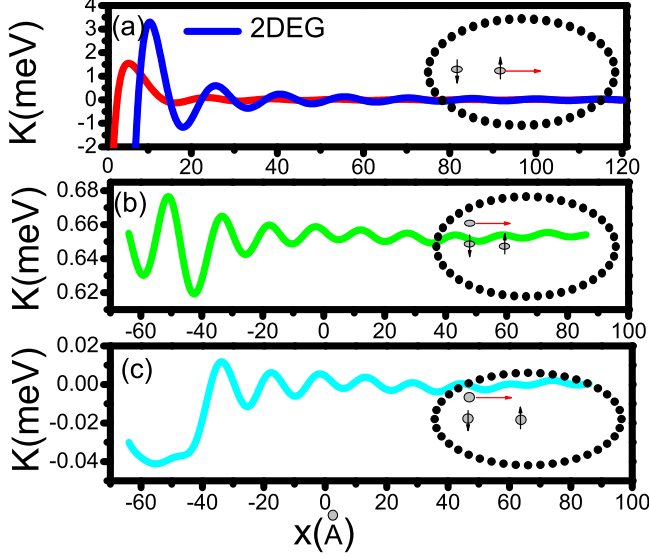


FIG. 1. (Color online) RKKY interaction between magnetic adatoms in a QC and nonmagnetic atom gating. (a) One of the magnetic atoms is moved along the x direction, while the other is kept fixed at the left focus, $x_c \approx 64 \text{ \AA}$ (red curve). The QC phase shifts and reduces the interaction in comparison with the free 2DEG (blue curve). (b) Two magnetic atoms are fixed at 1 nm separation, while a third nonmagnetic atom moves along the line $y = 1 \text{ nm}$. The RKKY interaction is strongly modulated when near the two magnetic adatoms. (c) RKKY for magnetic adatoms at 2.1 nm separation; the nonmagnetic atom gating greatly enhances as it sits few nm away from the magnetic pair. Notice different vertical scales in all panels. We have set $J = 0.2 \text{ eV}$ in all these plots.

each other (one at the left focus), while a third nonmagnetic atom is displaced inside the QC along a line 1 nm above the x -axis (i.e., $y = 1 \text{ nm}$), with x as indicated in the horizontal axis. The nonmagnetic atom can be seen to both enhance and suppress the RKKY interaction between the magnetic adatoms depending on its location, with a characteristic length scale of the Fermi wavelength in the 2DEG. Notice that when the gating atom is far away ($x > 2 \text{ nm}$), its effect is greatly diminished, as one could anticipate. In Fig. 1c, we see that even when the two magnetic impurities are held at 2.1 nm, and the corresponding RKKY interaction is much weaker, the presence of the gating atom enhances the effective exchange when nearby. This control of the effective interaction can be seen as arising from the modification of the single electron states in the 2DEG reservoir. As we will see below, the gating can also be shown to modify many body coherent states, as we illustrate by considering the Kondo effect.

We will now consider the gating effects on the competition between RKKY interaction and the Kondo effect. To this end, we consider the effective Hamiltonian $H = H_{\text{QC}} + H_{\text{imp}}$, where $H_{\text{imp}} = H_{\text{sd}} + H_{\text{RKKY}}$, to describe

the system, and focus here on the case of antiferromagnetic RKKY coupling, $K > 0$. To analyze this effective Hamiltonian, we employ a fermion representation of the spin operators $\vec{r}_i = (1/2)f_{i,s}^\dagger \vec{\sigma}_{s,s'} f_{i,s'}$, where the $\{f_{i,s}\}$ satisfy the constraint $f_{i,s}^\dagger f_{i,s} = 1$. A path integral representation of the partition function allows us to decouple the Kondo and RKKY interactions using Hubbard-Stratonovich fields $\{\chi_i\}$ and Φ , enforcing the fermion constraint with Lagrange multiplier fields $\{\lambda_i\}$. The decoupled effective Hamiltonian is then

$$H_{\text{imp}} = \sum_i \left[\lambda_i \left(f_{i,s}^\dagger f_{i,s} - 1 \right) + \frac{2}{J} |\chi_i|^2 - \chi_i^\dagger \psi_s^\dagger(\mathbf{R}_i) f_{i,s} - \chi_i f_{i,s}^\dagger \psi_s(\mathbf{R}_i) \right] + \frac{2}{K} |\Phi|^2 - \Phi f_{1,s}^\dagger f_{2,s} - \Phi^\dagger f_{2,s}^\dagger f_{1,s} . \quad (7)$$

To proceed further, we treat Eq. (7) in mean-field, so that the $\{\chi_i, \lambda_i, \Phi\}$ fields are taken to be c-numbers, to be determined self-consistently via (taking $\chi_i, \Phi \in \mathbf{R}$)

$$\chi_i = (J/2) \langle f_{i,s}^\dagger \psi_s(\mathbf{R}_i) + \psi_s^\dagger(\mathbf{R}_i) f_{i,s} \rangle , \quad (8a)$$

$$\Phi = (K/2) \langle f_{1,s}^\dagger f_{2,s} + f_{2,s}^\dagger f_{1,s} \rangle , \quad (8b)$$

$$1 = \langle f_{i,s}^\dagger f_{i,s} \rangle . \quad (8c)$$

The physical quantity of interest is the spectral function or local density of states (LDOS) in the QC^{11,17}

$$A(\mathbf{r}, \omega) = -(1/2\pi) \text{Im} [G(\mathbf{r}, \mathbf{r}; \omega)] , \quad (9)$$

where $G(\mathbf{r}, \mathbf{r}'; \omega)$ is the retarded GF in the QC, taking into account the two magnetic impurities

$$G(\mathbf{r}, \mathbf{r}'; \omega) = G_0(\mathbf{r}, \mathbf{r}'; \omega) + \sum_{i,j=1}^2 G_0(\mathbf{r}, \mathbf{r}_i; \omega) \hat{T}_{ij}(\omega) G_0(\mathbf{r}_j, \mathbf{r}'; \omega) , \quad (10)$$

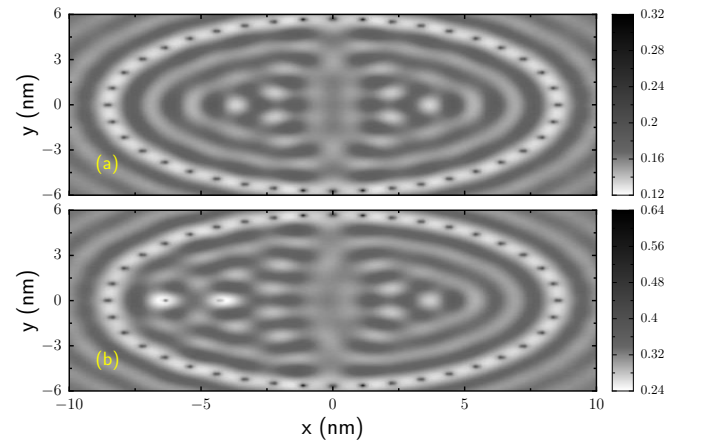


FIG. 2. Spatial scan of the LDOS at the Fermi energy. (a) Empty QC with no magnetic impurities. (b) QC with two magnetic impurities, one at the left focus, and the other one 2 nm away.

where $\hat{T}_{ij}(\omega)$ is the retarded GF at the impurity sites,

$$\hat{T}_{ij}(t) = -i\Theta(t)\langle\{f_{i,s}(t), f_{j,s}^\dagger\}\rangle \chi_i \chi_j. \quad (11)$$

As before, $G_0(\mathbf{r}, \mathbf{r}'; \omega)$ is determined by Eq. (6). We note that the \hat{T} matrix characterizes the magnetic order in the adatom system, as related to the fermion representation operator. In the case of a single impurity, for example, $\hat{T}(\omega)$ exhibits a clear resonance feature at/near the Fermi level (the Abrikosov-Suhl-Kondo resonance), of a width proportional to the Kondo temperature (energy scale) of the Kondo screening provided by the host electrons.¹¹

Figure 2 shows a spatial map of the QC's LDOS at the Fermi energy, for two different cases. Figure 2a shows the LDOS for the empty QC (no other adatoms), while Fig. 2b shows the influence of the two magnetic adatoms (separated 2 nm) on the LDOS. It is noticeable that the LDOS on the right side of the QC is nearly unchanged.

Two magnetic adatoms. Let us now discuss how single atom gating can modify the well known mirage signal in the QC.⁷ We discuss first gating with a magnetic adatom, so that we also explore how the competition between RKKY and Kondo interactions is ‘transmitted’ inside the QC. Figure 3 shows the spectral function $A(\vec{r}, \omega)$ (LDOS) at the empty (right) focus of the QC, $\vec{r} = (c, 0)$, for different configurations of the magnetic pair inside the QC. The inset shows the corresponding \hat{T}_{11} matrix. In all cases here, one adatom is placed at the left focus, $\vec{r}_1 = (-c, 0)$, while the second magnetic adatom is located at the \vec{r}_2 positions indicated by the label, displaced horizontally from the focus by 1, 2.1, and 5 nm (red, green, and blue curves, respectively). The main panel also shows results for an empty QC (‘no impurity’, dashed cyan curve), showing a featureless curve over the window shown, as it essentially measures the underlying 2DEG inside the QC. The LDOS for a single impurity at \vec{r}_1 (black dotted curve) shows a characteristic Fano lineshape at \vec{r}_1 ,³¹ associated with the Kondo resonance present in \hat{T}_{11} , as shown in the inset. In all cases, the signal at the empty focus carries the information on the global configuration of the adatoms in the QC. The resonance in \hat{T}_{11} and Fano curve in A are the experimental signatures in the differential conductance seen in the well-known mirage experiments.⁹

When the second magnetic adatom is placed with only 1 nm separation from the one at the left focus, their interaction is dominated by the host-mediated RKKY (antiferromagnetic at this distance, $K \approx 0.65$ meV, as seen in Fig. 1b). The formation of a strong local singlet between the two impurities destroys the Kondo resonance, as seen both by the nearly zero \hat{T}_{11} (red) curve in the inset, and the correspondingly small two features in the LDOS, which can be associated with the local singlet and triplet configurations of the two adatoms. As the second adatom moves away, the spectral functions display and increasing Kondo character: at 2.1 nm separation (green curves), the \hat{T}_{11} matrix is nonzero, but away from the Fermi energy, and the lineshape in the main frame starts

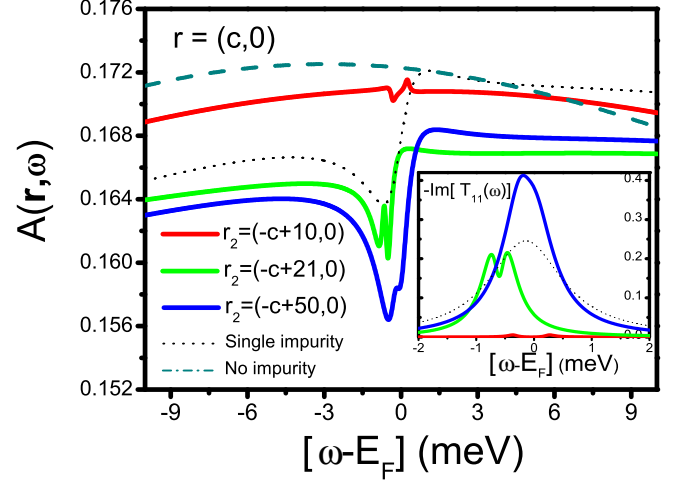


FIG. 3. Magnetic adatom gating of quantum mirage signal: RKKY vs Kondo competition. Spectral function A (LDOS) at the empty focus in the QC, $\vec{r} = (c, 0)$, as function of energy near the Fermi energy for different configurations. One adatom is held at left focus, $\vec{r}_1 = (-c, 0)$, while second is placed at \vec{r}_2 as labeled (10, 21, and 50 Å away). Inset shows corresponding \hat{T}_{11} vs energy. When close to each other, adatoms form a local singlet as RKKY dominates (red curves), while Kondo prevails at large separation (blue).

resembling the Fano form. At 5 nm separation (blue), the Kondo resonance is fully developed near the Fermi energy, with a width somewhat smaller than for the single impurity (dotted) case. Moving the second adatom further away results in a return to the single impurity case (not shown), as expected from the vanishing RKKY interaction at that distance. This figure illustrates that monitoring the empty focus reveals the competition between magnetic adatoms, be it a local singlet for strong RKKY pairing, or a well-resolved Kondo signal for large separation.

Nonmagnetic adatom gating. Figure 4 illustrates the effects of a nonmagnetic adatom used to gate the interaction between two magnetic adatoms in the QC. For this figure, we consider two magnetic adatoms kept 2.1 nm apart, with one of them at the left focus, $(-c, 0)$. The nonmagnetic adatom is then introduced at different locations, as indicated by the \vec{r}_3 label. In the absence of the gating atom, the RKKY interaction is relatively weak, as seen in Fig. 1a. When the nonmagnetic adatom is close to the magnetic impurity, at $\vec{r}_3 = (-c + 30, 10)$ Å, $K \approx -0.03$ meV. Correspondingly, \hat{T}_{11} in Fig. 4, pink curve, appears weak and with a split peak well below the Fermi energy, indicating the dominant role of the RKKY pairing. As the gating atom moves away, the RKKY is weakened further (see Fig. 1c), and the LDOS and \hat{T}_{11} show the characteristic Fano lineshape and Kondo resonance. In other words, even when the two magnetic

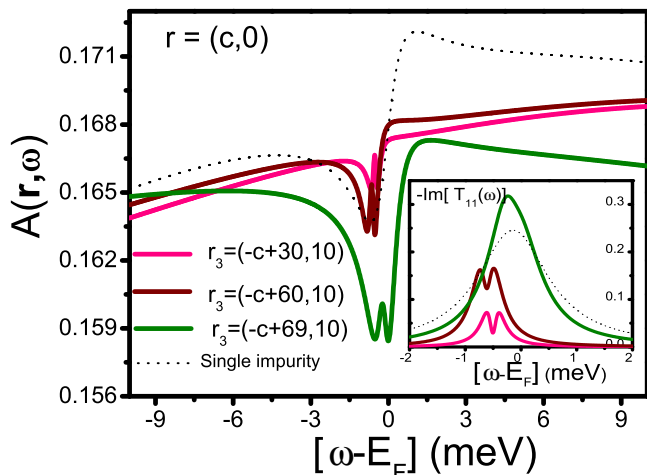


FIG. 4. Nonmagnetic atom gating regulates RKKY vs Kondo states. LDOS at the empty right focus, $\vec{r} = (c, 0)$, as function of energy, for different configuration of three adatoms. Two magnetic impurities are 2.1 nm apart, with one at the left focus. The third nonmagnetic adatom is placed at different locations, as indicated by \vec{r}_3 . When gating adatom is close to magnetic pair, the RKKY interaction dominates, causing only small features in LDOS and weak \hat{T}_{11} (pink curves). At larger separations, the RKKY nearly vanishes (see Fig. 1), and the Kondo screening of each impurity dominates, as seen clearly in the green curves.

impurities are relatively distant (or close), the gating adatom is able to enhance (suppress) the RKKY pairing and weaken (strengthen) the Kondo state of the adatom at the left focus. Moving the gating adatom further away in this case results in stable Kondo signatures.

These results exemplify the important role of gating adatoms in the QC as a way to control the effective interaction between magnetic impurities in the QC. The gating control has different character, depending on the magnetic character (or not) of the adatom, as well as on the relative configuration. The competition between

RKKY and Kondo screening provided by the host electrons can be modified thanks to the control of the corresponding single-particle and singlet many-body states involved. In that sense, one could see atomic gating as a way to modify the resulting entanglement of different adatom configurations.

We should comment that microscopic details of the adatom-surface combination used to implement these ideas would of course be important in direct comparison with experiments. Our model has ignored coupling to the (typically remote) bulk bands, which may affect the strength of the gating effect, since the bulk electrons would not be confined to the QC. Similarly, host lattice anisotropies may modify the isotropy of the RKKY interaction we have assumed, and introduce directional dependencies that would reinforce the gating effects. Finally, strong adatom hybridization may result in weaker magnetic moments, which may also reduce the RKKY or Kondo interactions. However, we believe that the large variety of experimentally accessible systems used to build and study QCs—such as cobalt adatoms on copper or gold surfaces—would allow for the successful implementation of these atom gating techniques.

To summarize, we have demonstrated how single gating atom effects enable precise control over the coupling between spin degrees of freedom in a quantum corral structure. We demonstrated that this coupling enables control over superpositions of many-body states, and, subsequently, the resulting stable configuration of magnetic impurities in the system. Although we have demonstrated this effect only on elliptical QCs, it is clear that such control could be implemented by the use of other ‘reflecting’ surfaces.³² We also notice that gating in such confined spaces is a more subtle non-additive effect, as would have been expected in open geometries. One could also imagine that this control over state superposition could find utility in various other systems. One could fabricate model systems for the investigation of low-dimensional magnetic assemblies with tunable interactions, or perhaps employ these approaches to control entanglement of different configurations of magnetic moments and implement spin-based computation schemes.

This work was supported by NSF-DMR grant 1508325 (Ohio).

¹ *Concepts in Spin Electronics*, S. Maekawa ed. (Oxford University Press, Oxford, 2006); *Semiconductor Spintronics and Quantum Computation*, D. D. Awschalom, D. Loss, and N. Samarth eds. (Springer, New York, 2002).

² S. A. Wolf, D. D. Awschalom, R. A. Buhrman, J. M. Daughton, S. von Molnár, M. L. Roukes, A. Y. Chtchelkanova, and D. M. Treger, *Science* **294**, 1488 (2001).

³ E. M. Vogel, *Nature Nanotech.* **2**, 25 (2007); N. Engheta, *Science* **317**, 1698 (2007); H. G. Craighead, *Science* **290**, 1532 (2000).

⁴ S. W. Hla, *Rep. Prog. Phys.* **77**, 056502 (2014).

⁵ M. F. Crommie, C. P. Lutz, and D. M. Eigler, *Science* **262**, 218 (1993).

⁶ D. M. Eigler, C. P. Lutz, M. F. Crommie, H. C. Manoharan, A. J. Heinrich, and J. A. Gupta, *Phil. Trans. R. Soc. Lond. A* **362**, 1135 (2004).

⁷ H. C. Manoharan, C. P. Lutz, and D. M. Eigler, *Nature* **403**, 512 (2000).

⁸ E. Rossi and D. K. Morr, *Phys. Rev. Lett.* **97**, 236602 (2006).

⁹ A. A. Aligia and A. M. Lobos, *J. Phys. Cond. Matt.* **17**, S1095 (2005).

- ¹⁰ J. D. Walls and E. J. Heller, *Nano Lett.* **7**, 3377 (2007).
- ¹¹ A. T. Ngo, J. Rodriguez-Laguna, S. E. Ulloa, and E. H. Kim, *Nano Lett.* **12**, 13 (2012).
- ¹² C. R. Moon, C. P. Lutz, and H. C. Manoharan, *Nature Phys.* **6**, 454 (2008).
- ¹³ P. G. Piva, G. A. DiLabio, J. L. Pitters, J. Zikovsky, M. Rezeq, S. Dogel, W. A. Hofer, and R. A. Wolkow, *Nature* **435**, 658 (2005).
- ¹⁴ J. Martínez-Blanco, C. Nacci, S. C. Erwin, K. Kanisawa, E. Locane, M. Thomas, F. von Oppen, P. W. Brouwer, and S. Fölsch, *Nature Phys.* **11**, 640 (2015).
- ¹⁵ C. Rössler, D. Oehri, O. Zilberberg, G. Blatter, M. Karalic, J. Pijnenburg, A. Hofmann, T. Ihn, K. Ensslin, C. Reichl, and W. Wegscheider, *Phys. Rev. Lett.* **115**, 166603 (2015).
- ¹⁶ L. S. Rodberg and R. M. Thaler, *Introduction to the Quantum Theory of Scattering* (Academic Press, New York, 1967).
- ¹⁷ G. A. Fiete, E. J. Heller, *Rev. Mod. Phys.* **75**, 933 (2003).
- ¹⁸ A. C. Hewson, *The Kondo Problem to Heavy Fermions* (Cambridge University Press, Cambridge, 1993).
- ¹⁹ V. Madhavan, W. Chen, T. Jamneala, M. F. Crommie, and N. S. Wingreen, *Science* **280**, 567 (1998).
- ²⁰ J. Li, W.-D. Schneider, R. Berndt, and B. Delley, *Phys. Rev. Lett.* **80**, 2893 (1998).
- ²¹ M. A. Ruderman and C. Kittel, *Phys. Rev.* **96**, 99 (1954); T. Kasuya, *Prog. Theor. Phys.* **16**, 45 (1956); K. Yosida, *Phys. Rev.* **106**, 893 (1957).
- ²² C. F. Hirjibehedin, C. P. Lutz, and A. J. Heinrich, *Science* **312**, 1021 (2006).
- ²³ L. Zhou, J. Wiebe, S. Lounis, E. Vedmedenko, F. Meier, S. Blügel, P. H. Dederichs, and R. Wiesendanger, *Nature Phys.* **6**, 187 (2010).
- ²⁴ A. A. Khajetoorians, J. Wiebe, B. Chilian, S. Lounis, S. Blügel, and R. Wiesendanger, *Nature Phys.* **8**, 497 (2012).
- ²⁵ E. S. Sørensen and I. Affleck, *Phys. Rev. B* **53**, 9153 (1996).
- ²⁶ H. Prüser, P. E. Dargel, M. Bouhassoune, R. G. Ulbrich, Th. Pruschke, S. Lounis, and M. Wenderoth, *Nature Commun.* **5**, 5417 (2014).
- ²⁷ A. Allerdtd, C. A. Büsser, G. B. Martins, and A. E. Feiguin, *Phys. Rev. B* **91**, 085101 (2015).
- ²⁸ C. Kittel, *Quantum Theory of Solids*, Ch. 18 (John Wiley & Sons, New York, 1963).
- ²⁹ I. S. Gradshteyn and I. M. Ryzhik, *Table of Integrals, Series, and Products* (Academic Press, San Diego 1994).
- ³⁰ A. A. Correa, F. A. Reboredo, and C. A. Balseiro, *Phys. Rev. B* **71**, 035418 (2005).
- ³¹ O. Újsághy, J. Kroha, L. Szunyogh, and A. Zawadowski, *Phys. Rev. Lett.* **85**, 2557 (2000).
- ³² C. Trallero-Giner, S. E. Ulloa, and V. López-Richard, *Phys. Rev. B* **69**, 115423 (2004).
- ³³ This implicitly assumes that if present, surface-induced magnetic anisotropy leaves a degenerate low-energy doublet in each magnetic impurity that behaves as an effective spin-1/2 system.